Photoneutron Cross Sections for ^{24}Mg, ^{26}Mg, and Natural Magnesium†

S. C. Fultz, R. A. Alvarez, B. L. Berman, M. A. Kelly,* D. R. Lasher, and T. W. Phillips
Lawrence Radiation Laboratory, University of California, Livermore, California 94550

and

J. McElhinney
U. S. Naval Research Laboratory, Washington, D. C. 20390
(Received 7 December 1970)

Photoneutron cross sections for ^{24}Mg, ^{26}Mg, and natural magnesium have been measured with the use of monochromatic photons obtained from the annihilation in flight of fast positrons. The resolution was less than 200 keV at 10-MeV photon energy, and 300 keV at 30 MeV. About 14 resonant structures in ^{24}Mg and 32 in ^{26}Mg were distinguished and parametrized. A Porter-Thomas treatment of the distributions of transition widths throughout the giant resonances of ^{24}Mg and ^{26}Mg indicates that the resonances belong to single-spin states, or have one degree of freedom in each case. The ^{26}Mg$(\gamma, 2n)$ cross section contains considerable structure, most of it coinciding with the structure in the total photoneutron cross section. It is confirmed that the giant resonance of ^{26}Mg is split into two isospin components. Integrated total cross sections up to 28 MeV are 50 MeV mb for ^{24}Mg, 226 MeV mb for ^{26}Mg, and 76 MeV mb for natural magnesium.

I. INTRODUCTION

Photoneutron and photoproton cross sections have been measured previously for magnesium isotopes and natural magnesium. The majority of work has been conducted on natural magnesium, however, which makes it difficult to compare with data taken with separated isotopes. Adequate references to earlier works are contained in several bibliographies.[1] More recent work has revealed the presence of numerous levels in the giant resonance of some of the magnesium isotopes. This is seen as complex structure in the cross section. The structure has been studied by means of (γ, n), (γ, p), and (e, e') reactions. It has also been examined by the inverse reaction ^{23}Na$(p, \gamma_0)^{24}$Mg.[2]

For ^{24}Mg, Nathans and Yergin[3] obtained an integrated cross section of 55 MeV mb, up to 25 MeV. King and McDonald[4] obtained approximately 31.5 MeV mb up to 24.7 MeV for $\sigma((\gamma, n) + (\gamma, pn) + 2(\gamma, 2n))$ on ^{24}Mg. Using the absorption method, Dolbilkin *et al.*[5] obtained a total absorption integrated cross section of 365 $^{+40}_{-20}$ MeV mb for $\sigma((\gamma, n) + (\gamma, pn) + (\gamma, 2n) + (\gamma, p))$, while Wyckoff *et al.*[6] obtained 276 MeV mb for this integrated total cross section up to 30 MeV.

Min and Whitehead[7] measured $\sigma((\gamma, n) + (\gamma, pn) + 2(\gamma, 2n))$ using the neutron counting method and natural magnesium. They obtained an integrated cross section of 90.7 MeV mb for energies up to 28 MeV. Anderson, Cook, and Englert,[8] using the activation method, obtained an integrated cross section for $\sigma((\gamma, n) + (\gamma, 2n))$ of approximately 92 MeV mb for energies up to 28 MeV for ^{24}Mg.

Some measurements have been made on the (γ, p) cross section for ^{24}Mg. Ishkhanov *et al.*[9] obtained 180 MeV mb for integrated cross sections of this reaction up to 32 MeV, while Shoda *et al.*[10] obtained 70 MeV mb for this cross section up to 23 MeV. The most detailed of the photoproton studies is the (p, γ_0) yield data of Bearse, Meyer-Schutzmeister, and Segel,[2] but the resulting ^{24}Mg(γ, p_0) cross section is such a small branch of the giant-resonance decay (~1.5%) that it cannot be considered to be representative of the whole, and consequently a comparison with the conclusions of Bearse *et al.* (such as the ratio of "direct" to compound-nucleus decay of the giant resonance) is not meaningful.

The separated isotopes ^{24}Mg and ^{26}Mg have been examined by electron scattering by Titze *et al.*,[11-13] who measured structure in ^{24}Mg and ^{26}Mg (e, e') cross sections. Photoneutron spectra also have been measured for these isotopes.[14-17] The results on the separated isotopes obtained at other laboratories will be discussed later in this report.

Theoretical calculations on the giant-dipole-resonance levels in ^{24}Mg have been made by Nilsson, Sawicki, and Glendenning[18] using the random-phase approximation in a deformed harmonic oscillator. Diehl, Forkman, and Steifler[19] modified these calculations, while Neudatchin and Shevchenko[20] included consideration of the monopole part of the Majorana force in their calculation of the $1d$-$2s$ shell nuclei. Bassichis and Scheck[21] applied a Hartree-Fock treatment in their calculation of resonances in the ^{24}Mg nucleus. No calculations on ^{26}Mg have been reported to date.

The previous measurements of the photoneutron cross sections for the magnesium isotopes and natural magnesium, obtained at other laboratories, show considerable disagreement in absolute values and in detail of the structure. The present work was undertaken in an attempt to present a more coherent picture of these cross sections for the various magnesium isotopes, using the higher-resolution data obtained by use of monochromatic photons. Single-nucleon effects were studied by use of the separated isotopes, and neutron multiplicity counting was used to separate the partial cross sections.

II. EXPERIMENTAL APPARATUS AND METHOD

The source of radiation was monochromatic photons obtained from the annihilation in flight of fast positrons.[22] The energy range of the annihilation photons was from approximately 10 to 28 MeV. The photon beam was measured by means of an ion chamber, filled with xenon gas to a pressure of 0.5 atm. It was calibrated by correlating the charge collected from the ion chamber with intensity of annihilation photons as measured by an 8-in.×8-in.-diam NaI(Tl) crystal. For the calibration measurements, response functions were fitted to the peaks in the pulse-height distributions obtained from the NaI(Tl) crystal, and the total counts under the response function were obtained.

The sample was placed at the center of a 3-in.-diam axial hole in a 4π paraffin-moderated neutron detector. The detector contained 48 BF_3 proportional counters, each filled to a pressure of 160 cm Hg with ^{10}B-enriched (to 96%) BF_3. The paraffin moderator consisted of a 24-in. cube of paraffin, with the BF_3 tubes placed in four rings arranged concentrically around the axis of the cylindrical hole.

TABLE I. Threshold energies for magnesium isotopes (MeV) (from Ref. 23).

Isotope	(γ,n)	$(\gamma,2n)$	(γ,pn)	(γ,p)
^{24}Mg	16.532	29.940	24.112	11.694
^{25}Mg	7.329	23.881	19.022	12.061
^{26}Mg	11.095	18.424	23.156	14.147

The ^{26}Mg sample consisted of 79.12 g of MgO with the ^{26}Mg enriched to 99.70%. The weight of ^{26}Mg in the sample was 50.04 g. It was packed in a thin-walled 1.75-in.-diam Lucite container which was placed at the center of the axial hole in the neutron detector. Two ^{24}Mg samples were used. One was oxide in chemical form and consisted of 98.17 g of ^{24}MgO enriched to 99.88% ^{24}Mg. The second sample consisted of ^{24}Mg metal having an enrichment of 99.91% ^{24}Mg. The metal was contained in small irregular drops, and was packed in a thin-walled Lucite container. The natural magnesium sample consisted of a number of machined metal disks, 1.5-in. diam and 0.25 in. thick. These were stacked into a cylinder taped together and placed at the center of the neutron detector. Various weights of natural magnesium were used depending on which group of resonances was being examined. Threshold energies for several photon reactions are shown in Table I.[23]

Two arrangements of the beam transport system were used for the measurements on the magnesium

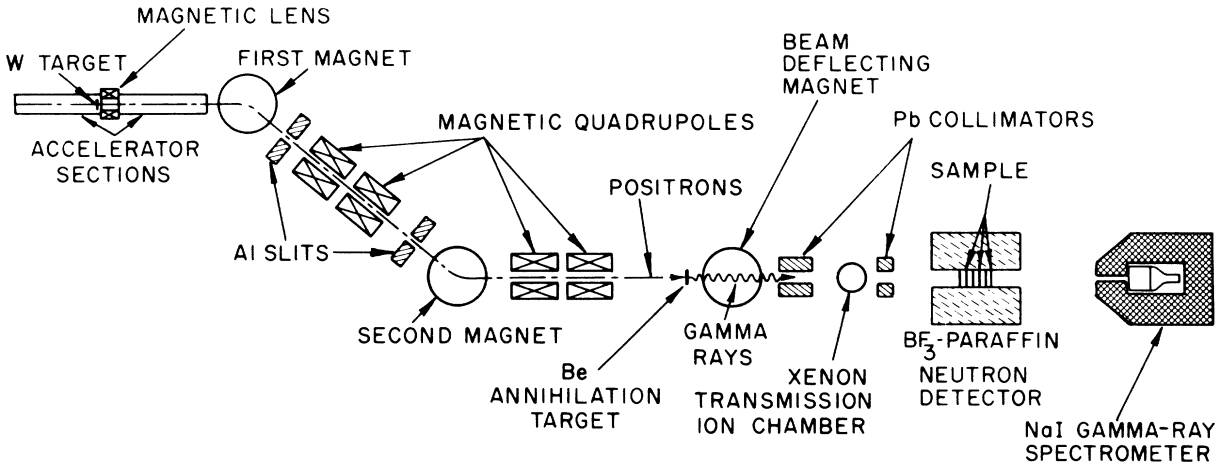

FIG. 1. Arrangement of the beam-handling equipment and experimental apparatus used for the ^{24}Mg and natural-magnesium measurements. The ^{26}Mg data were obtained with the arrangement shown in Fig. 1 of Ref. 24.

TABLE II. Integrated cross sections of magnesium isotopes.

Isotope	$\int_{E_{thr}}^{28} \sigma(\gamma, n_{tot})dE$ (MeV mb)	$\int_{E_{thr}}^{28} \sigma(\gamma, 2n)dE$ (MeV mb)
^{24}Mg	50	...
^{26}Mg	226	68
Natural magnesium	76	...

isotopes. The first, with which natural magnesium and ^{24}Mg were measured, is shown in Fig. 1. The second system, with which ^{26}Mg, ^{25}Mg, and ^{23}Na were measured, is shown in Fig. 1 of the work of Alvarez *et al.*,[24] which is a report on the latter two isotopes. In both arrangements, the beam was focused on a beryllium annihilation target by a final quadrupole. The annihilation target consisted of a 0.5-in.-diam disk of beryllium metal, 0.010 in. thick, suspended on thin nylon threads and mounted in a target changer which could be operated remotely. The target changer consisted of a thin Synthane wheel of approximately 12-in. diam. A number of 2.25-in.-diam holes with centers on a 7.5-in.-diam circle were made in the wheel. In these could be mounted targets of various sizes and thicknesses which could be positioned in the beam line with high accuracy. When background measurements were desired, a hole with no target was rotated into the beam line.

A fine wire was attached to each target and a potential of 270 V was placed between the target and an electrically isolated collector electrode mounted inside the vacuum chamber. The total charge collected from the target during a run was measured along with that obtained from the transmission ion chamber. Thus, the targets could be used as secondary emission monitors, and the data supported the readings of the charge collected from the ion chamber. The positron beam transmitted by the annihilation target finally was bent out of the beam line and arrested in carbon blocks.

The method of measurement has been discussed in other reports.[22,24] It consisted of observing the neutron counts at selected energies of annihilation photons for a chosen amount of charge obtained from the ion chamber. The fields of all magnets then were reversed and neutron counts were observed for a similar charge from the ion chamber for negative electrons. The neutron counts were

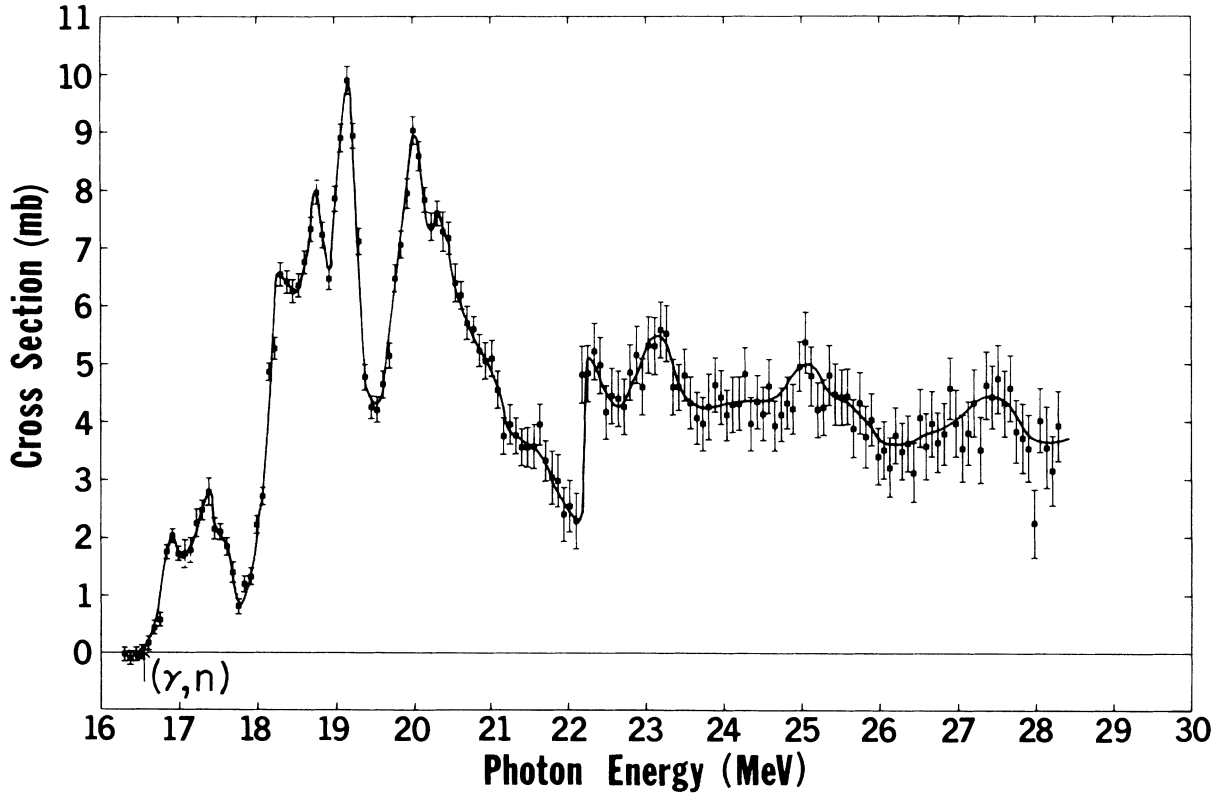

FIG. 2. Total photoneutron cross section $\sigma((\gamma,n)+(\gamma,pn))$ for ^{24}Mg. The solid line is drawn merely to guide the eye.

TABLE III. Analytical and experimental resonance energies for ^{24}Mg (MeV).

Resonance number	Analytical energy	Experimental energies: Present data (γ, n_{tot})	Livermore (Ref. 15) (γ, n_0)	Yale (Ref. 14) (γ, n_0)	Darmstadt (Ref. 12) (e, e')	Argonne (Ref. 2) (γ, p_0)
1	16.92	16.90	16.871		16.90	16.9
			16.95		17.08	17.2
2	17.32	17.30	17.30		17.33	17.35
3	17.55	17.65	17.83	17.83	17.60	17.5
				17.95	17.90	
				18.15	18.21	
4	18.33	18.30	18.26	18.36	18.50	18.25
5	18.75	18.82	18.61	18.58	18.85	18.5
6	19.16	19.17		19.21	19.23	19.0
				19.48		19.3
7	20.00	20.05		19.95	20.10	20.1
8	20.40	20.36			20.35	20.4
9	20.80	20.90			20.77	20.7
					21.16	
10	21.45	21.45			21.50	
11	22.35	22.35			22.28	
12	23.10	23.10			23.02	
					23.42	
13	25.00	25.00			25.05	
14	27.50	27.50				

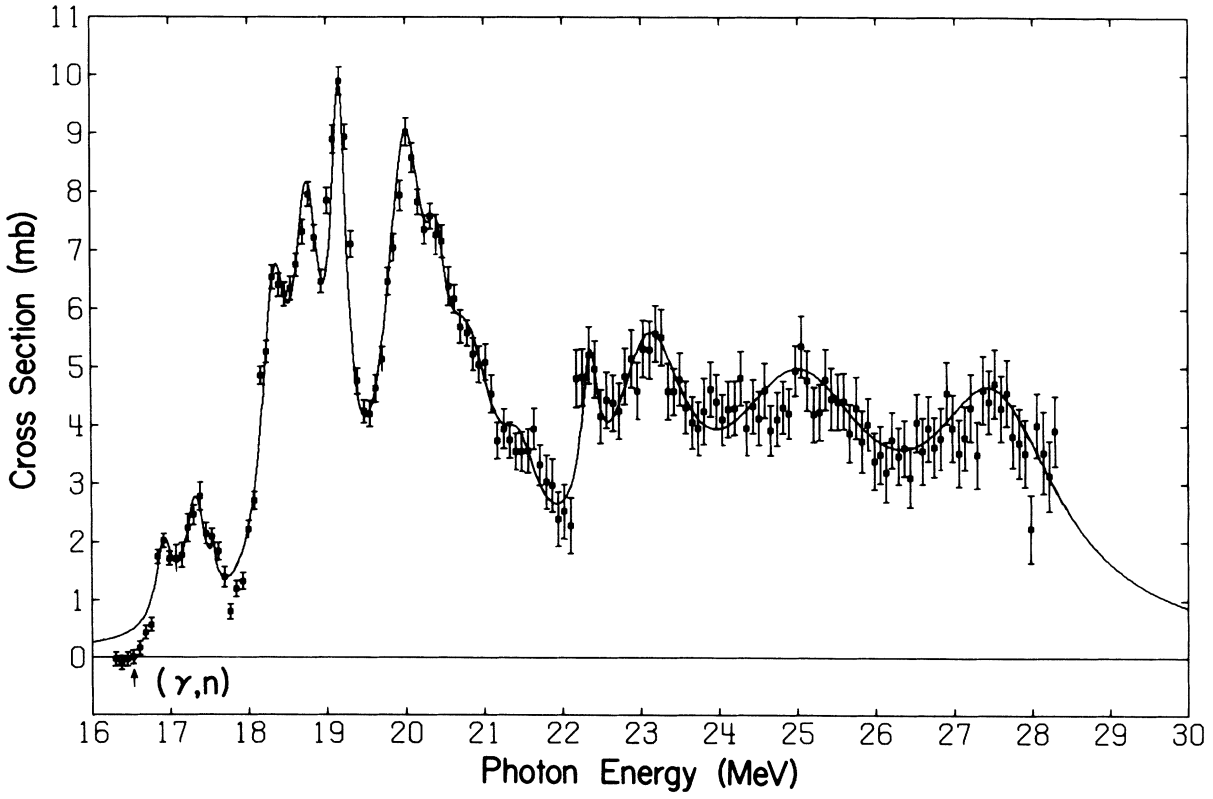

FIG. 3. ^{24}Mg total cross section $\sigma((\gamma,n)+(\gamma,pn))$ fitted with a calculated cross-section curve. The solid line is the sum of the 14 Lorentz lines whose parameters were adjusted to fit the data.

normalized to the same number of particles, and the negative electron data were subtracted from the positron data.

The efficiency of the neutron detector was approximately 0.40. The neutron counts were analyzed electronically so that single, double, triple, etc. counts per beam burst were separated and counted on separate scaling circuits. From these data the particle cross sections $\sigma((\gamma, n)+(\gamma, pn))$ and $\sigma(\gamma, 2n)$ were calculated on a computer, using a statistical analysis. Since the average energy of the neutrons changes with a change in the incident photon energy, the efficiency of the neutron detector was measured as a function of the neutron energy, by use of the "ring-ratio" method.[25] Corrections for neutron detector efficiency were applied to the data.

The resolution of the photon beam varied from less than 200 keV at 10 MeV to 300 keV at 30 MeV.[26] The momentum interval selected by the slit setting was approximately 1%, but other factors such as multiple scattering and energy loss in the beryllium target and the energy-versus-angle relation of the photon beam contributed to a loss of resolution at the lower energies.

III. EXPERIMENTAL RESULTS AND ANALYSIS

A. ^{24}Mg

The cross section $\sigma((\gamma, n)+(\gamma, pn))$ for ^{24}Mg is shown in Fig. 2. It reaches a maximum of 9.9 mb at 19.16 MeV, and considerable structure is present throughout the giant resonance. The integrated cross section for photon energies up to 28 MeV is 50 MeV mb. This can be compared with other magnesium isotopes in Table II. The energies of the peaks in the cross-section curve are shown in Table III. Also listed in Table III are data from the Livermore,[15] Yale,[14] Darmstadt,[12] and Argonne[2] nuclear laboratories. The Livermore[15] and Yale data were obtained by the neutron time-of-flight method, the Darmstadt data are from inelastic electron scattering measurements, and the Argonne data are from (p, γ_0) measurements.

The data were analyzed by fitting Lorentz lines to the peaks and summing these to reproduce the cross-section curve. This was done by use of a computer, and the parameters of the Lorentz lines were chosen to give the best fit to the measured cross-section curve. In Fig. 3 are shown the cross-section data and the curve obtained by summing the Lorentz lines. Integrated cross sections (areas) for the Lorentz lines are given in Table IV.

The cross section for absorption of a photon having energy E from the ground state to an excited state at energy E_k is given by the expression

$$\sigma(E)=4\pi\lambda_k^2\, g\frac{\gamma_{k0}}{\Gamma_k}\,\frac{(E\Gamma_k)^2}{(E_k^2-E^2)^2+(E\Gamma_k)^2}, \qquad (1)$$

where γ_{k0} is the ground-state radiative transition width and Γ_k is the total width of the level observed: $\Gamma_k=\Gamma_{nk}+\gamma_{k0}+\sum_i\gamma_{ki}+\Gamma_{pk}$, where γ_{ki} are the non-ground-state radiative widths.

The widths Γ_{pk}, for the (γ, p) reaction, are not known and will be omitted in the present analysis. (This is not expected to change the level distribution but would increase the values of γ_{k0} by approximately a factor of 2, since $\Gamma_{pk}\simeq\Gamma_{nk}$.) The λ_k are the wavlengths of the incident photons, and the Γ_k are measured experimentally. For dipole radia-

TABLE IV. Resonance parameters and integrated cross sections for ^{24}Mg.

Resonance number "k"	Energy E_k (MeV)	Total width Γ_k (MeV)	Relative dipole strength ϕ_k	Integrated cross section $\int_0^\infty\sigma\,dE$ (MeV mb)	Radiative transition width γ_{k0} (eV)
1	16.92	0.27	0.097	0.59	14.6
2	17.32	0.32	0.167	1.04	27.0
3	17.55	0.07	0.009	0.057	1.5
4	18.33	0.40	0.463	3.04	88.6
5	18.75	0.42	0.575	3.86	117.7
6	19.16	0.26	0.415	2.85	90.7
7	20.00	0.63	1.000	7.16	248.5
8	20.40	0.30	0.145	1.06	38.2
9	20.80	0.80	0.590	4.40	164.9
10	21.45	0.60	0.194	1.49	59.5
11	22.35	0.25	0.123	0.98	42.7
12	23.10	1.15	0.870	7.20	333.0
13	25.00	2.40	1.700	15.22	825.0
14	27.50	2.00	1.180	11.62	762.0

tion on an even-even nucleus $g = \frac{3}{2}$, when taking into account the two possible directions of polarization. Since the γ_k are small compared to Γ_n, we get

$$\int_0^\infty \sigma dE = 2\pi^2 \lambda\!\!\!^{-2} g \gamma_{k0} ,$$

whence

$$\gamma_{k0} = \int_0^\infty \sigma dE/(3\pi^2 \lambda\!\!\!^{-2}) . \qquad (2)$$

Equation (2) was used to calculate the radiative widths of the various resonances whose Lorentz parameters were obtained in the manner previously described. The values obtained for γ_{k0} are listed in the right column of Table IV.

B. ^{26}Mg

The partial cross sections $\sigma((\gamma, n) + (\gamma, pn))$ and $\sigma(\gamma, 2n)$ and the total photoneutron cross section $\sigma((\gamma, n) + (\gamma, pn) + (\gamma, 2n))$ for ^{26}Mg are shown in Figs. 4–6, respectively. The data show marked structure throughout the giant-resonance region. Among the significant features of these data is the appearance of two dominant peaks (at approximately 17.6 and 22 MeV) in the total-cross-section curve. Only one of these (at 17.6 MeV) appears clearly in the (γ, n) cross section (Fig. 4), while the other appears in the $(\gamma, 2n)$ cross section (Fig. 5). The apparent splitting in the giant resonance will be discussed later in this report.

The total cross section reaches its first maximum of 22.8 mb at 17.65 MeV and its second maximum of 25.1 mb at 22.14 MeV. The $(\gamma, 2n)$ cross section has a maximum of 13.9 mb at 21.9 MeV. Considerable structure also is apparent in the $(\gamma, 2n)$ cross section curve; however, statistics are not quite as good here as for the single or total photoneutron measurements. However, the energies of the peaks agree reasonably well with those of resonances 18 to 23, 25, and 27, respectively, of Table V. Also listed in Table V are energies at which peaks were observed in ^{26}Mg(γ, n_0) measurements made at Livermore[15] and at Yale,[17] as well as those from electron scattering data from Darmstadt.[13]

The second column of Table V is a list of the energies used in analysis of the Livermore data in which a Lorentz line was fitted to each peak in the cross-section curve. The entries in this column differ a little from the experimental data of the

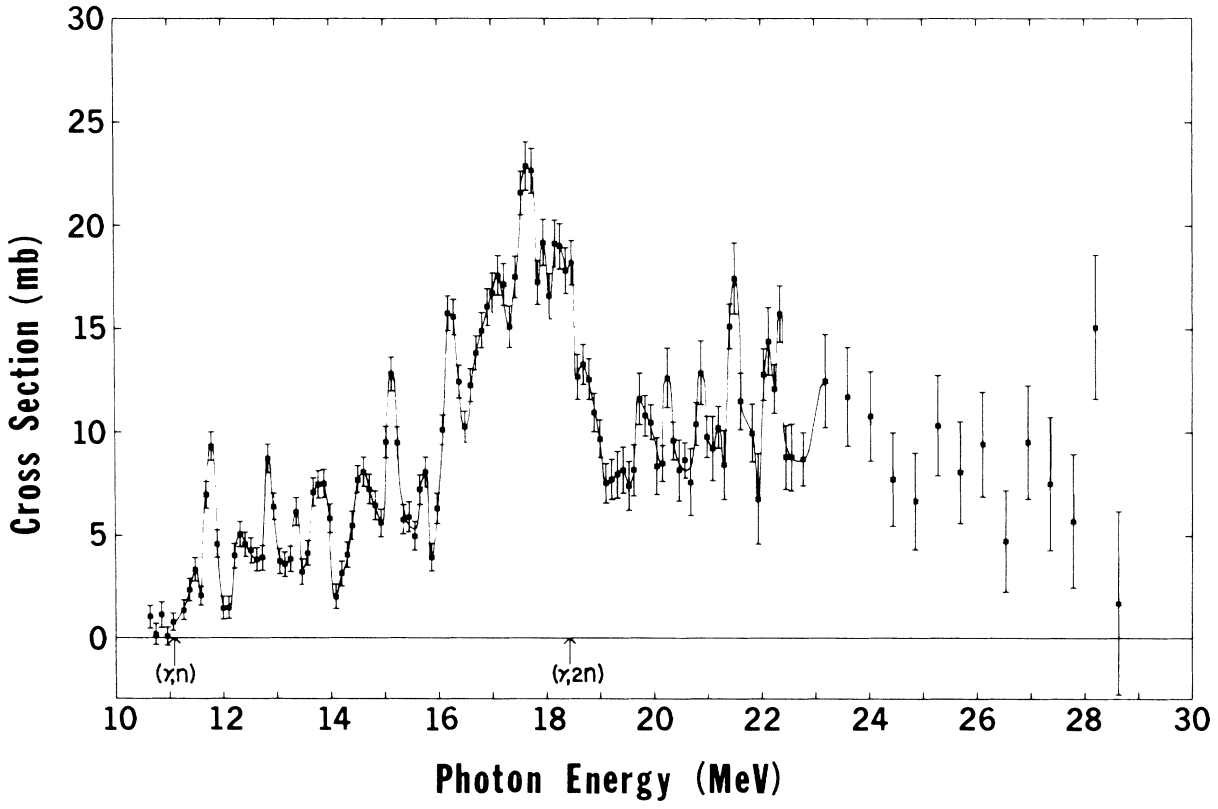

FIG. 4. Single-photoneutron cross section $\sigma((\gamma,n) + (\gamma,pn))$ for ^{26}Mg.

third column, since the tails of adjacent resonance lines will shift the peaks slightly. In addition, where wide spacings occurred between peaks, it sometimes was necessary to add Lorentz lines which did not appear in the experimental data (as peaks) in order to account for all the cross section. In Fig. 7 is shown the cross-section curve obtained by summing these lines.

Using Eq. (2), the γ-ray transition widths γ_{k0} were calculated for ^{26}Mg from the areas under the Lorentz lines. These are listed in the right column of Table VI. The integrated cross sections for each line are given in the fifth column, while relative dipole strengths are listed in the fourth column.

C. Natural Mg

The total photoneutron cross section for natural magnesium is shown in Fig. 8. The structure below 16.5 MeV is mostly attributable to ^{26}Mg, since there is little structure apparent in ^{25}Mg in this region.[24] The resonances occur at energies of 11.80, 12.28, 12.90, 13.35, 13.83, 14.70, 15.27, 15.68, and 16.35 MeV, and are identifiable with resonances 3 to 11, inclusive, of ^{26}Mg as listed in Table V. The resonances above 16.35 MeV, which appear at 16.90, 17.52, 18.30, 18.77, 19.17, 20.00, 20.32, and 20.95, are readily identifiable with ^{24}Mg; namely resonances 1, 2, and 4 through 9 of Table III.

The total cross section rises to a peak value of approximately 10 mb at 19.17 MeV, and has an integrated value of 76 ± 7 MeV mb, up to 28 MeV. The integrated cross section obtained from the sums of the isotopic cross sections, taking into account isotopic abundances, is 88 ± 9 MeV mb. These are in agreement within the statistical errors. (The integrated cross section of ^{25}Mg was taken as 226 MeV mb.[24])

IV. DISCUSSION AND CONCLUSIONS

A. Integrated Cross Sections

The integrated cross section for ^{24}Mg from the present data is 50 ± 5 MeV mb. It is difficult to compare this with other experiments, since many experimenters used natural magnesium, and the cross sections were listed as due to ^{24}Mg. How-

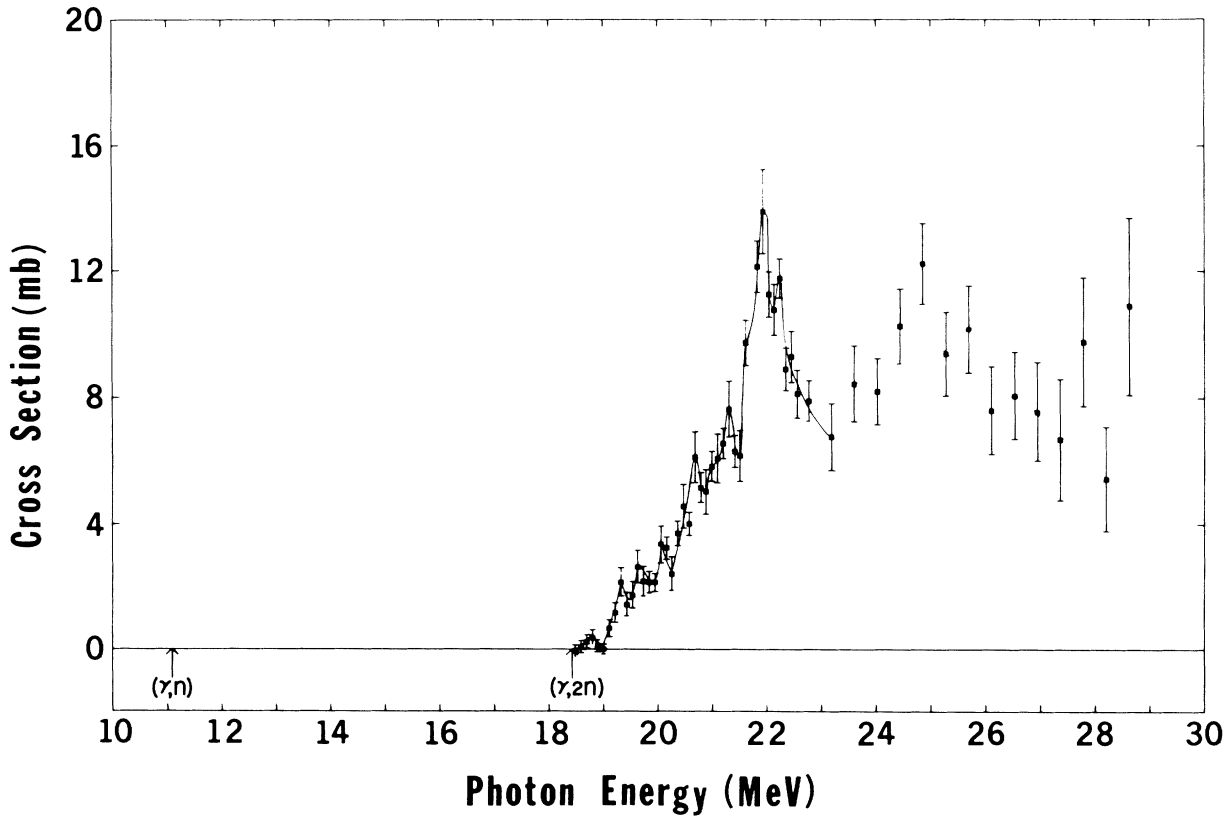

FIG. 5. Double-photoneutron cross section $\sigma(\gamma, 2n)$ for ^{26}Mg.

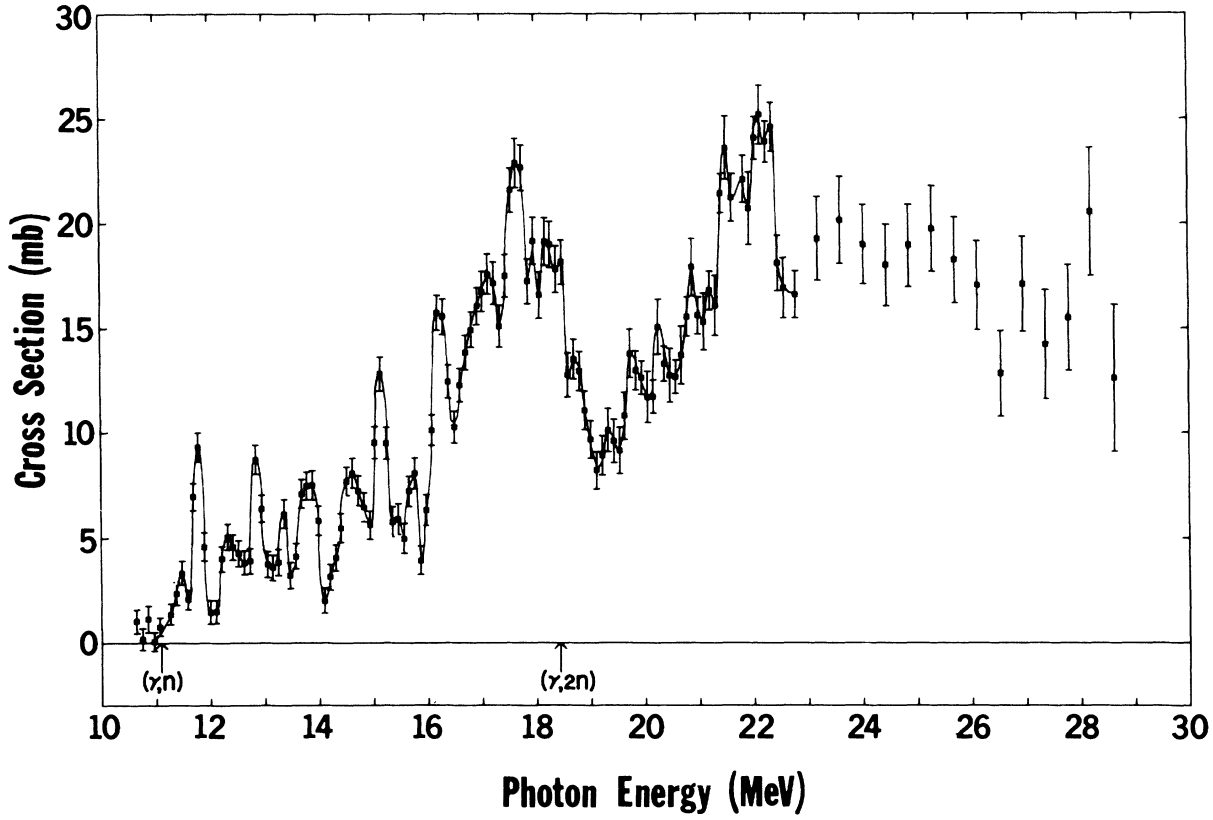

FIG. 6. Total photoneutron cross section $\sigma((\gamma,n)+(\gamma,pn)+(\gamma,2n))$ for ^{26}Mg. The solid line is used only to guide the eye.

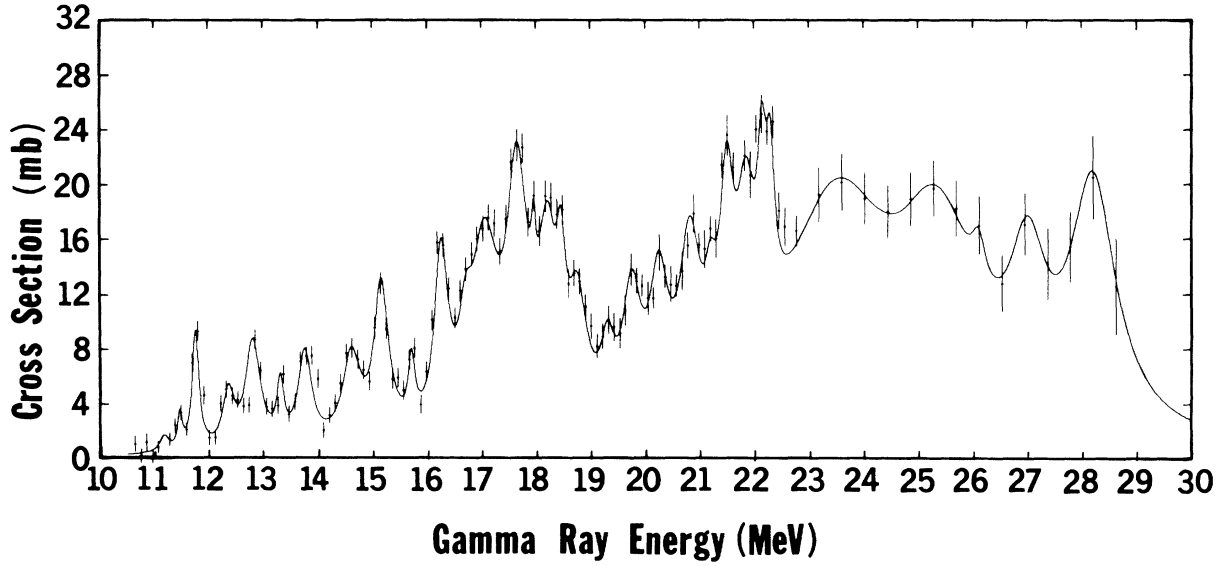

FIG. 7. Total photoneutron cross section $\sigma((\gamma,n)+(\gamma,pn)+(\gamma,2n))$ for ^{26}Mg. The solid line is the sum of 32 Lorentz lines with parameters listed in Table VI.

ever, summing the contributions from the isotopes ^{24}Mg, ^{25}Mg, and ^{26}Mg gives a total integrated cross section which is in reasonable agreement with the measurement on natural Mg, as previously noted.

The first moment of the integrated cross section $\sigma_{-1} = \int_0^\infty \sigma E^{-1} dE$ is proportional to the sum of the dipole strengths ϕ_k given in Tables IV and VI. It is 2.79 mb for ^{24}Mg and 12.1 mb for ^{26}Mg.

B. Nuclear Deformation

Some measurements have been made on the intrinsic quadrupole moment of ^{24}Mg and of β_2, the nuclear deformation[27]:

$$\beta_2 = \frac{2}{3}\left(\frac{\pi}{5}\right)^{1/2} \epsilon ,$$

where ϵ is the eccentricity:

$$\epsilon = (a^2 - b^2)/R^2 ,$$

TABLE V. Analytical and experimental resonance energies for ^{26}Mg (MeV).

				Experimental energies		
				Livermore	Yale	Darmstadt
Resonance number	Analytical energy	Present data (γ, n_{tot})	$(\gamma, 2n)$	(Ref. 15) (γ, n_0)	(Ref. 17) (γ, n_0)	(Ref. 13) (e, e')
1	11.17	11.15		11.155		
				11.164		
				11.289		
				11.333		
2	11.46	11.47		11.511		
3	11.75	11.75		11.753		
4	12.35	12.30		12.279		
5	12.80	12.80			12.81	
					12.90	
					13.04	13.12
6	13.30	13.35			13.33	13.35
					13.44	
7	13.75	13.75			13.67	13.70
		13.83				13.89
						14.22
8	14.60	14.60			14.49	14.50
						14.91
9	15.15	15.15			15.10	15.12
10	15.70	15.70			15.59	15.73
11	16.25	16.20				16.25
12	16.70	16.70				16.90
13	17.05	17.15				17.16
14	17.65	17.65				17.52
15	17.95	17.95				17.83
16	18.20	18.20				18.19
17	18.45	18.45				18.51
18	18.75	18.75	18.80			18.79
19	19.30	19.30	19.32			19.21
20	19.75	19.75	19.63			19.66
21	20.25	20.25	20.05		20.37	20.12
22	20.82	20.87	20.68		20.77	20.59
23	21.20	21.30	21.30		21.16	21.09
24	21.50	21.50			21.37	21.42
25	21.85		21.93			21.93
26	22.15	22.15			22.13	
27	22.30		22.25			22.74
28	23.50	23.00				23.15
			24.9			23.60
29	25.35	25.25				
30	26.10					
31	27.00	27.00				27.32
32	28.20	28.20				

TABLE VI. Resonance parameters and integrated cross sections for ^{26}Mg.

Resonance number "k"	Energy E_k (MeV)	Total width Γ_k (MeV)	Relative dipole strength ϕ_k	Integrated cross section, $\int_0^\infty \sigma\, dE$ (MeV mb)	Radiative transition width γ_{k0} (eV)
1	11.17	0.20	0.085	0.37	4.0
2	11.46	0.10	0.09	0.40	4.5
3	11.75	0.15	0.45	2.04	24.4
4	12.35	0.25	0.33	1.57	20.8
5	12.80	0.33	0.82	4.05	57.5
6	13.30	0.15	0.19	0.99	15.1
7	13.75	0.30	0.60	3.18	52.2
8	14.60	0.40	0.70	3.94	72.9
9	15.15	0.32	0.96	5.61	112.
10	15.70	0.15	0.18	1.09	23.3
11	16.25	0.30	0.94	5.89	135.
12	16.70	0.30	0.35	2.25	54.5
13	17.05	0.60	1.85	12.17	307.
14	17.65	0.45	1.80	12.25	331.
15	17.95	0.10	0.11	0.73	20.
16	18.20	0.40	1.05	7.37	212.
17	18.45	0.20	0.34	2.42	71.
18	18.75	0.40	0.70	5.06	154.
19	19.30	0.30	0.28	2.08	67.
20	19.75	0.40	0.72	5.48	186.
21	20.25	0.40	0.73	5.70	203.
22	20.82	0.45	1.00	8.03	302.
23	21.20	0.25	0.22	1.80	70.
24	21.50	0.30	0.72	5.97	239.
25	21.85	0.40	0.82	6.91	286.
26	22.15	0.20	0.39	3.33	142.
27	22.30	0.17	0.29	2.49	108.
28	23.50	2.40	7.15	64.8	3104.
29	25.35	1.75	3.70	36.2	2016.
30	26.10	0.30	0.15	1.5	89.
31	27.00	0.80	1.20	12.5	790.
32	28.20	1.00	2.50	27.2	1875.

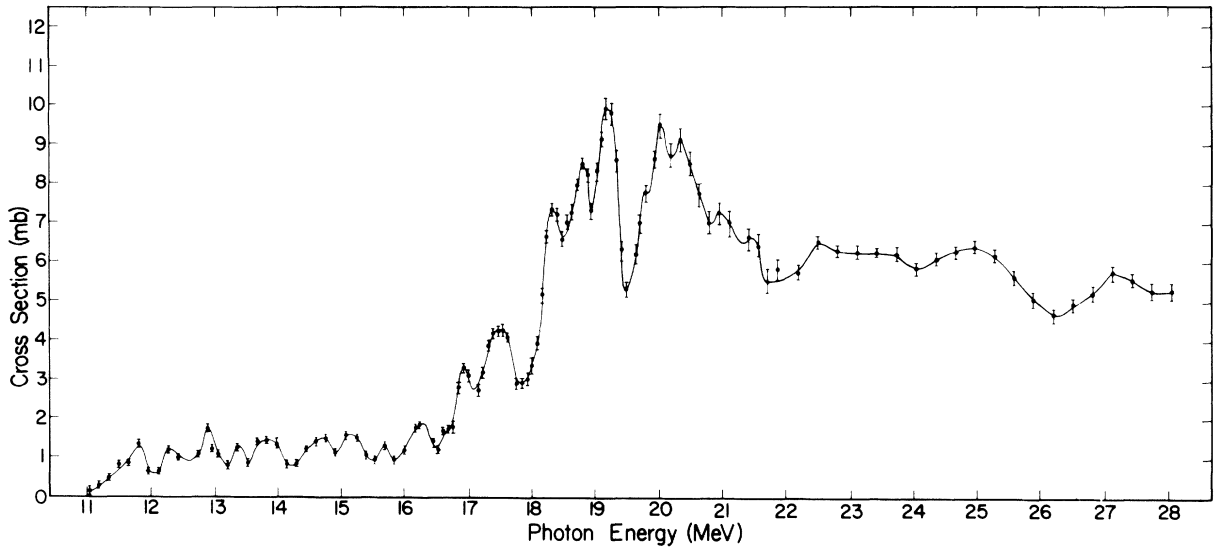

FIG. 8. Natural magnesium total cross section $\sigma((\gamma,n)+(\gamma,pn)+(\gamma,2n))$ showing detailed structure. The solid line is merely to guide the eye through the data points.

where a and b are semimajor and semiminor axes of a prolate spheroid, and R is the equivalent spherical radius.

The average value of β_2 for ^{24}Mg, based on a number of measurements, is given[27] as 0.65 from which $\epsilon = 1.230$. From early work on electron scattering,[28] $R = 3.84$ F, so for ^{24}Mg we get $a = 5.21$ F and $b = 3.30$ F, or $a/b = 1.58$. If the ^{24}Mg nucleus is regarded as deformed, giving low- and high-energy components in the cross section, and the low-energy component is regarded as centered about 17 MeV,[18] the high-energy maximum would be expected to occur at approximately 26 MeV. Although the cross section appears to be still (relatively) strong in the region around 26 MeV, no marked peaks occur there.

A theoretical treatment by Nilsson, Sawicki, and Glendenning[18] of the giant resonance in the deformed s-d shell employed the random-phase approximation with Nilsson wavefunctions and Ferrel-Fisscher and Rosenfeld forces for the residual interaction. The calculated dipole strengths showed a splitting between the $K = 0$ and $K = 1$ resonances, but the distribution of dipole strength disagrees with the experimental data. Bassichis and Scheck[21] applied the static Hartree-Fock self-consistent-field calculation to the $1p$, the $2s, 1d$, and the $2p, 1f$ shell. They, too, obtained a splitting of the dipole strength for the $K = 0$ and $K = 1$ cases. For comparison with the present experiment, some of their results are shown in Table VII, wherein dipole strengths greater than 0.1 are shown for the energy range above the (γ, n) threshold. The great strength predicted at 26.65 MeV does not appear in the present data, and far too little dipole strength is attributed to the region below 22 MeV. A somewhat better distribution appears in the work of Neudatchin and Shevchenko,[20] who took into account the difference in binding energy of a nucleon in the outer unfilled shell and in the closed shell. The relative dipole strengths they obtained are shown in Table VIII. It can be seen that the strength appears to be more evenly spread throughout the giant-resonance region, but still there is not satisfactory agreement with the present data.

The ^{26}Mg cross section (Fig. 6) shows marked structure and the possibility of several groupings of the levels. It is not obvious which groups of levels, if any, are a consequence of the influence of nuclear deformation on the cross section. However, an estimation of the excitation-energy difference between groups of levels excited in a deformed ^{26}Mg nucleus is of interest. The deformation[27] β_2 for ^{26}Mg is 0.52, which gives an energy ratio of 1.47 for the two groups of levels. Thus, if the low-energy group were centered about 17 MeV, the high-energy group would be centered about 25 MeV. Unfortunately, no detailed theoretical treatment has been published for the ^{26}Mg nucleus, so no comparison with theory is possible.

C. Resonance Analysis

The data presented in this report appear sufficiently detailed that application of statistical treatments should yield further insight into the properties of the giant resonances of the magnesium isotopes examined. The resonances in the cross sections were analyzed by fitting to them Lorentz curves, the parameters for which are given in Tables IV and VI. (The total cross section was then synthesized by adding the contribution of each Lorentz line.) The close agreement between the present data and that from other laboratories or experiments (some of which were taken at higher resolution), indicates that the resonances do not overlap strongly (except in the wings). That few levels appear to have been missed, up to a certain energy limit, will be demonstrated in treatments below. Hence even though it would be expected that the resonances would each represent a level (or several levels) with the same spin and parity ($J^\pi = 1^-$),

TABLE VII. Calculated relative dipole strengths for ^{24}Mg transitions (from Ref. 21).

$K = 0$		$K = 1$	
Energy (MeV)	f_{0n}	Energy (MeV)	f_{0n}
27.50	0.15	29.75	1.99
23.04	2.40	28.23	0.23
21.78	0.15	26.65	15.86
21.25	0.41	23.63	1.10
18.52	2.52	22.64	0.34
		18.12	0.43
		17.44	0.48
		16.75	0.53

TABLE VIII. Calculated relative dipole strengths for ^{24}Mg transitions (from Ref. 20).

Energy (MeV)	f_{0n}
18.2	3.0
18.6	5.0
20.7	3.0
21.1	3.5
22.0	3.5
25.0	5.5
27.0	7.0
28.0	8.0
29.5	3.0
30.5	4.6

for the present analysis these resonances are not considered to interfere. They therefore are treated as each representing a single level with Lorentzian shape.

Experimental resolution prevents us from knowing whether all the resonances are single levels or clusters of levels (all 1^- states) akin to doorway states.[29] However, regardless of whether they are single levels or groups of levels, the analytical methods of statistical analysis developed for neutron resonances would be expected to be applicable. A Porter-Thomas[30] analysis has therefore been applied. This is a model-independent treatment which merely gives the distribution of the ground-state transition widths, based upon the number of channels (or degrees of freedom) through which the nucleus may be excited. Other analytical treatments of the data yield such valuable information as (a) the $E1$ strength functions, (b) the energy limit up to which no appreciable number of levels are missed, and (c) the average resonance spacing.

1. ^{24}Mg

A plot of a running sum $\sum_k \gamma_{k0}$ of radiation widths versus photon energy is given in Fig. 9. From the slope of this curve can be deduced an average value for the strength function $\langle \gamma/D \rangle$. For ^{24}Mg we thus get $\langle \gamma/D \rangle = 196 \times 10^{-6}$, where D is the level spacing.

In Fig. 10 is given a plot of the number of resonances contained in the energy interval between the (γ, n) threshold and the photon energy E_γ. This represents a "lost level" diagram. When the resolution becomes very poor and "levels" thus are being missed, this curve deviates from a straight line cutting the abscissa at the threshold energy. It is evident that such levels are being lost at energies above 21.5 MeV. For those below this energy, the slope of the straight line gives an average value for the number of levels per MeV of excitation energy, or $\langle 1/D \rangle$, where D is the level spacing. From the figure we get $\langle 1/D \rangle = 1.89$ MeV^{-1} or $\langle D \rangle = 0.528$ MeV. Thus, the average ground-state radiation width for these ^{24}Mg excited states is $\langle \gamma \rangle = \langle \gamma/D \rangle \langle D \rangle$, or $\langle \gamma \rangle = 104$ eV. These values for $\langle \gamma \rangle$ and $\langle D \rangle$ apply to the resonance structures actually observed. However, the average value obtained for the strength function $\langle \gamma/D \rangle$ should be independent of the resolution.

It is of interest to examine the distribution of widths of the photon transitions to excited states in the giant-resonance region of ^{24}Mg. To do this we consider the distribution function deduced by Porter and Thomas[30]:

$$P(x, \rho)dx = (\rho x)^{\rho-1} e^{-\rho x} dx/\Gamma(\rho), \tag{3}$$

where $P(x, \rho)$ is the probability of a transition width falling in the range between x and $x + dx$, $x = \gamma/\langle \gamma \rangle$ is the ratio of γ to the average width $\langle \gamma \rangle$, $\nu = 2\rho$ is a parameter known as the number of degrees of freedom, and $\Gamma(\rho)$ is the Γ function.

A plot of $P(x, \rho)$ for the levels of ^{24}Mg listed in Table IV is given in Fig. 11 wherein the histogram represents the experimental data, and the solid lines are the theoretical width-distribution curves for ρ values of $\frac{1}{2}$ and 1, or ν values of 1 and 2. The histogram appears to agree more closely with the theoretical curve for $\nu = 1$, or a single degree of freedom. The average value of ν obtainable from this data can be calculated from the expression given by Wilets[31]:

$$\nu_{\text{eff}} = \frac{2\langle \gamma \rangle^2}{\langle \gamma^2 \rangle - \langle \gamma \rangle^2}. \tag{4}$$

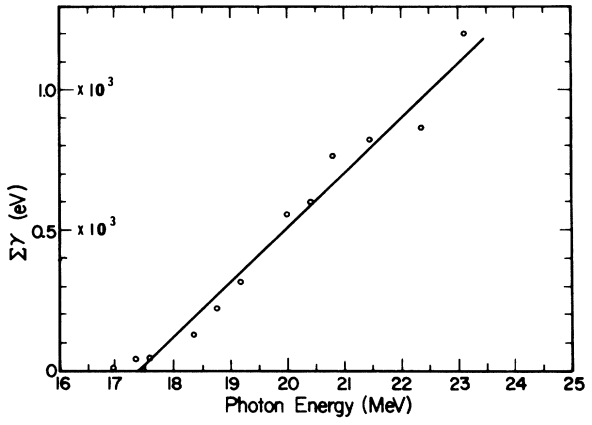

FIG. 9. The data points are running sums of the transition widths γ_k plotted versus the excitation energy for ^{24}Mg.

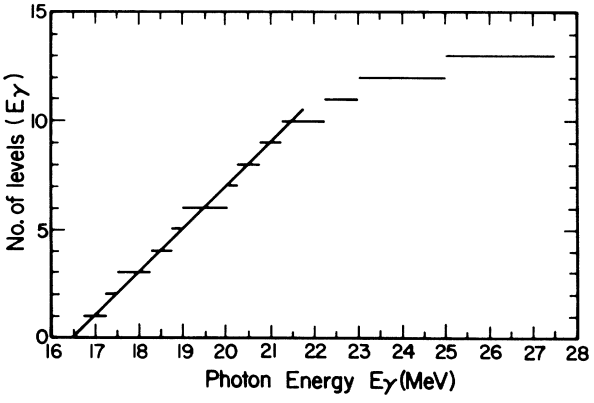

FIG. 10. "Lost level" diagram for ^{24}Mg. This gives the number of levels with energy less than E_γ, plotted versus E_γ.

Using this expression, we get

$$\nu_{\text{eff}} = 1.21 .$$

Alternatively, using the expression[30]

$$F(\rho) = \psi(\rho) - \ln\rho , \tag{5}$$

where $\psi(\rho)$ is the derivative of the logarithm of the Γ function and

$$F(\rho) = (1/m)\sum_{i=1}^{m} \ln(x_i) ,$$

we get

$$\rho = 0.668 \pm 0.021$$

or

$$\nu = 1.34 \pm 0.04 .$$

Both calculations of ν are in reasonable agreement and indicate ν to be close to unity. This is consistent with the histogram in Fig. 11.

Since ^{24}Mg is a self-conjugate nucleus, its ground state has isospin $T = 0$. Hence, only $T = 1$ states can be reached by dipole excitation. Transitions from these states to $T = \frac{1}{2}$ states of ^{23}Mg are allowed by isospin selection rules. However, it is not known whether all the excited states apparent in the ^{24}Mg cross section decay to the ground state of ^{23}Mg. The appearance of the same resonances in the neutron spectra[14,15] of the (γ, n_0) reaction on ^{24}Mg from threshold to 3.45 MeV, however (see Table III) indicates that up to an excitation energy of approximately 20 MeV the resonances seen in the total photoneutron cross section (Fig. 2) are associated with ground-state transitions. The neutron decay from the strong resonances at 16.9, 17.3, 18.3, 18.8, and 19.2 MeV can be shown to proceed essentially entirely to the ground state of ^{23}Mg by converting the differential cross sections given in Refs. 14 and 15 to total cross sections, even though decay to the 0.45-MeV first excited state of ^{23}Mg is possible for all but the lowest of these resonances. In addition, the close correlation of the time-of-flight data with the (γ, n) and (e, e') measurements indicates that most of the resonances are accounted for in the present measurements on ^{24}Mg, as is indicated in Fig. 10.

Since electric dipole radiation can excite only $J^{\pi} = 1^{-}$ states in ^{24}Mg, there would be expected only one degree of freedom for the resonances observed in the ^{24}Mg nucleus. Hence, best agreement with a Porter-Thomas distribution of the level widths would be expected for $\nu = 1$. This appears to be the case (Fig. 11), and the calculated value of ν has an average value of 1.28 [Eqs. (4) and (5)].

2. ^{26}Mg

A plot of the number of resonances occurring in ^{26}Mg between the (γ, n) threshold and photon energy E is shown in Fig. 12. This lost-level plot indicates that most of the levels below 22 MeV are accounted for in the data. Comparison with photoneutron data taken near threshold by Berman *et al.*[15,16] at Livermore, indicates that a few peaks near threshold were missed. A comparison of the values for γ_{k0} found in Ref. 15 and the present experiment (Table VI) discloses that the 11.15-MeV peak includes four levels, but resonances 2,

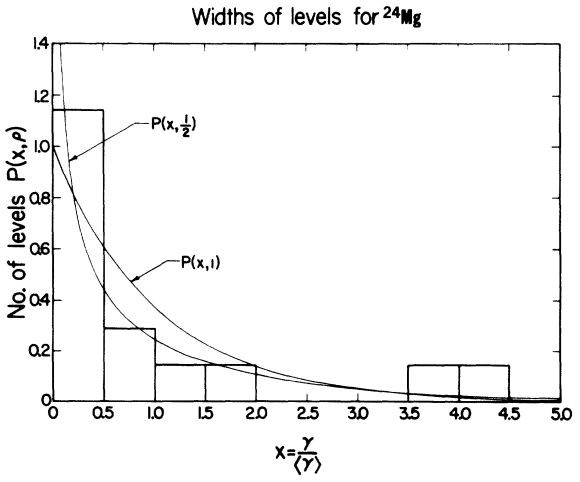

FIG. 11. Distribution of level widths $P(x,\rho)$ versus $x = \gamma/\langle\gamma\rangle$ for ^{24}Mg. $P(x,\rho)$ is given in Eq. (3), and $2\rho = \nu$ is the number of degrees of freedom. $P(x,\rho)$ is the fraction of levels in a bin $dx = 0.5$, normalized to $dx = 1$.

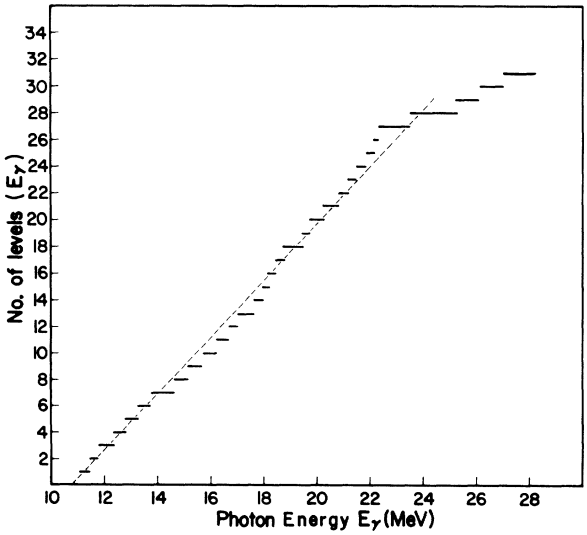

FIG. 12. Number of levels with energies less than E_γ versus photon energy E_γ for ^{26}Mg.

3, 4, and 5 in Table V are indeed single levels. Also, resonance 3 (11.75 MeV) decays essentially entirely to the ground state of ^{25}Mg; resonance 4 (12.3 MeV) decays to the ground state about 50% of the time, and resonance 5 (12.8 MeV), seen in the threshold photoneutron measurement as an excited-state transition, decays to the second excited state of ^{25}Mg (at 0.975 MeV) about 30% of the time. Finally, the agreement with the data from other laboratories (Table V) indicates that most of the peaks above 13.3 MeV of excitation energy are accounted for. From the reciprocal of the slope, $\langle D \rangle$ was found to be 0.473 MeV.

In Fig. 13 is shown a graph of a running sum of the transition widths versus photon energy. A distinct change in slope occurs at about 16.2 MeV, which gives two values for $\langle \gamma/D \rangle$. The region below 16.2 MeV yields a value for $\langle \gamma/D \rangle$ of 97×10^{-6}, while that above 16.2 MeV gives 438×10^{-6}. These numbers yield average transition widths of 45.9 and 207 eV, respectively, for the two energy regions.

The distribution of the levels $P(x,\rho)$, as defined by Eq. (3), was determined for the ^{26}Mg data and is shown in the histogram of Fig. 14. As in the previous case, the curves are the theoretical width distribution for ρ values of $\frac{1}{2}$ and 1, or ν values of 1 and 2, respectively. The histogram appears to agree more closely with the thoretical curve for $\nu=1$, for a single degree of freedom. The average value of ν deduced from Eq. (5) is

$$\nu = 1.03 \pm 0.24 .$$

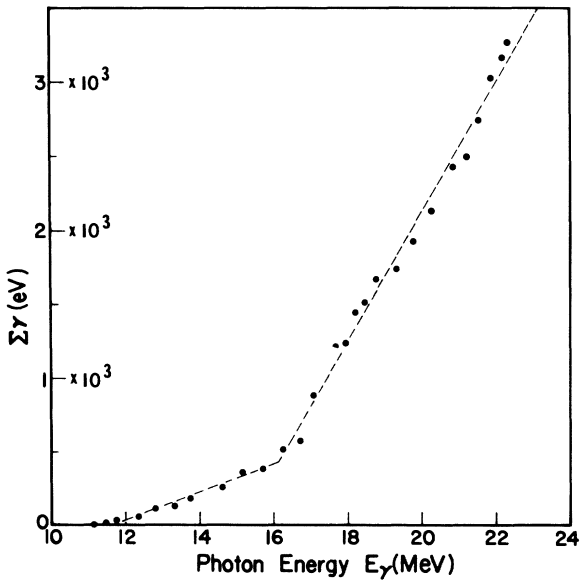

FIG. 13. The data points are running sums of transition widths γ_k plotted versus excitation energy for ^{26}Mg.

The Porter-Thomas treatment of the resonances of ^{26}Mg indicates a single dominant mode of exciting the levels in the giant resonance, i.e., a single degree of freedom. As before, this would be expected from dipole excitation of an even-even nucleus, since only $J^\pi = 1^-$ states would be excited.

The apparent change in the value of $\langle \gamma/D \rangle$ from 97×10^{-6} to 438×10^{-6} at 16.2 MeV (Fig. 13) appears to arise from the greater strength of the levels within the giant resonance proper, the start of which would be at about 16.2 MeV. Thus this kind of analysis gives a quantitative estimate of a lower-energy limit to the giant resonance when the cross section contains much structure. Under favorable conditions (non-overlapping resonances, good experimental energy resolution at 30 to 40 MeV), it would likewise be possible to extract an upper energy limit. It is hard to see how else one could set such energy limits on the giant resonance in cases like these where it is fragmented into many substructures.

D. Isospin Splitting of the Giant Resonance in ^{26}Mg

Interesting information on the ground-state neutron transitions from ^{26}Mg has been provided by the time-of-flight-measurements of Wu, Firk, and Berman.[17] These experimenters irradiated ^{26}Mg with bremsstrahlung having end-point energies of 18.9, 21.4, 23.1, and 27.5 MeV. The spectra then were normalized and subtracted. Of particular significance is the fact that neutron groups appearing for excitation energies greater than 18.9 MeV were reduced in energy by approximately 7.9 MeV.

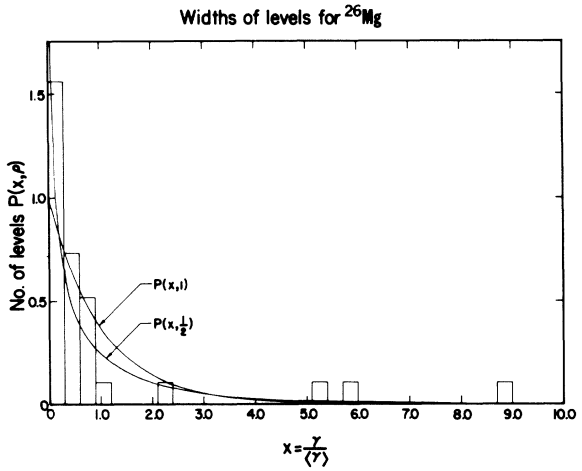

FIG. 14. Distribution of level widths $P(x,\rho)$ versus $x=\gamma/\langle\gamma\rangle$ for ^{26}Mg. $P(x,\rho)$ is the fraction of levels in a bin $dx=0.3$, normalized to $dx=1$.

Thus, there are no ground-state neutrons from states with energies between 18.9 and 23.1 MeV even though strong photon absorption occurs there (Fig. 6). This signifies that deexcitation of the ^{26}Mg levels in this energy range must occur by neutron emission to $T=\frac{3}{2}$ levels of ^{25}Mg, as indicated in Fig. 15. Since the ground state of ^{26}Mg has $T=1$, dipole radiation can excite levels with isospin $T=1$ or $T=2$. $T=2$ levels would decay only to $T=\frac{3}{2}$ levels in ^{25}Mg. Hence, levels in the range of 18.9 to 23.1 MeV must belong to a group having $T=2$. A pair of levels in ^{25}Mg at energies of 7.793 and 7.873 MeV are known to be $T=\frac{3}{2}$ levels.[32] The splitting of these levels appears in the neutron spectra measurements of Wu *et al.* which identifies them with the energies of excitation above 18.9 MeV.

Above the $(\gamma, 2n)$ threshold (18.42 MeV), there is sufficient energy left in the residual nucleus to deexcite by ejection of a second neutron, but deexcitation of $T=2$ levels in the energy range between 18.42 and 18.89 MeV must occur by a transition from a $T=2$ level to a $T=\frac{1}{2}$ level by neutron emission. Such a transition is forbidden by the T-selection rule. Since the first $T=\frac{3}{2}$ levels in ^{25}Mg require approximately 18.9-MeV excitation, transitions below this energy could only remain highly forbidden. Thus, the low $(\gamma, 2n)$ cross section

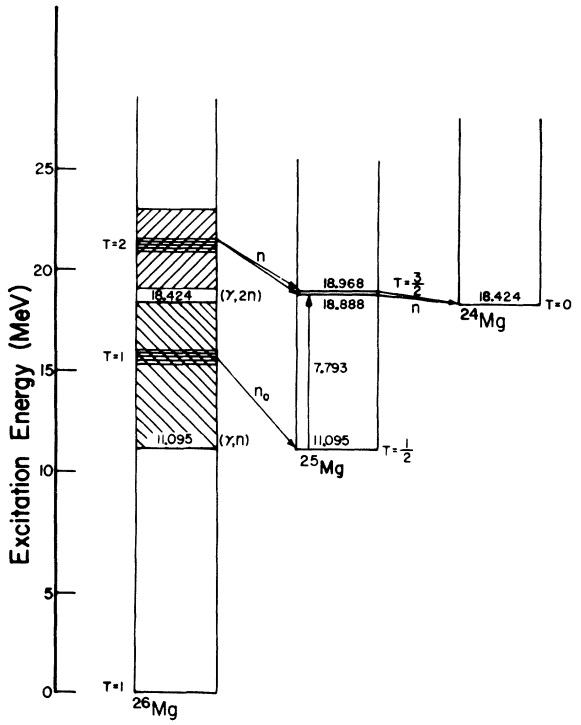

FIG. 15. Energy level relationships for the nuclei ^{24}Mg, ^{25}Mg, and ^{26}Mg.

just above threshold and until an excitation energy above 18.9 MeV is reached confirms the $T=2$ assignment of the states in this energy region.

The deexcitation of the $T=\frac{3}{2}$ levels in ^{25}Mg must occur through emission of a neutron to a $T=0$ level at or near the ground state of ^{24}Mg. (This must occur since the first $T=1$ level in ^{24}Mg is at approximately 9 MeV above the ground state.) Such a transition is also forbidden by T-selection rules. An explanation must be sought through mixing of the isospins of the $T=\frac{3}{2}$ levels of ^{25}Mg with $T=\frac{1}{2}$ components. This has been discussed by Berman, Baglan, and Bowman,[32] in which it is shown that the $T=\frac{3}{2}$ levels at 7.793 and 7.873 MeV are not absolutely pure, and such mixing does occur. Above the excitation energy required for emission of two neutrons, single-neutron emission from ^{26}Mg still can occur because of γ-ray emission from the $T=\frac{3}{2}$ doublet in ^{25}Mg, in competition with the emission of a second neutron. Thus, the ratio of the integrated cross sections for $\sigma(\gamma, n)$ to $\sigma(\gamma, 2n)$ [above the $(\gamma, 2n)$ threshold] represents roughly the ratio of the probabilities of decay of this doublet by γ-ray and neutron emission, i.e., the ratio of $\langle\gamma\rangle$ to $\langle\Gamma_n\rangle$. From Figs. 4 and 5, it appears to be approximately unity. This is in agreement with the previous observation[32] that the lower limit for this ratio is about 0.7.

The present work, combined with that of Wu, Firk, and Berman,[17] establishes a grouping of the dipole states of ^{26}Mg, whereby those below about 18 MeV have $T=1$ and those above 18.4 MeV and below at least 23 MeV have $T=2$. Such a grouping agrees with the theory of Fallieros[33] (for a spherical nucleus), who predicted that the separation between these two groups should be approximately 5 MeV for ^{26}Mg. This agrees with the present data if the centroids for the two groups are taken to be about 17 and 22 MeV. This grouping also was observed by Titze, Goldmann, and Spamer[13] from electron scattering data on ^{26}Mg.

The ratio of the integrated cross sections for the $T=2$ group to the $T=1$ group appears to be approximately 2 (Fig. 6) if the cross section above 23 MeV is included in the $T=2$ group. However, the isospin sum rule of O'Connell, Gibson, and Hayward[34] predicts that this ratio should be only 0.8. This might be explained if the cross section immediately above about 23 MeV does not arise from $T=2$ states, but rather from another, possibly overlapping, concentration of $T=1$ strength which was displaced through the deformation of the ground state. In a similar manner, one might expect a fourth concentration of strength centered about 5 MeV above the short-axis deformation peak in the cross section (at 25 MeV), at about 30 MeV. Further measurements are needed to

examine this concept of double splitting.

V. SUMMARY

The photoneutron cross sections for ^{24}Mg and ^{26}Mg have been measured with monochromatic γ rays, having energies up to 28 MeV and a resolution of approximately 2%. The cross sections have considerable structure throughout the giant-resonance region in both cases. The energies of the observed peaks agree well with those obtained from electron scattering and from neutron time-of-flight data. The distributions of the radiative transition widths of ^{24}Mg and ^{26}Mg were examined by means of a Porter-Thomas analysis and have been shown to agree closely with those expected for a single degree of freedom in both cases. Most of the transitions through neutron emission from ^{24}Mg excited states up to 20 MeV appear strongly in the ground-state cross section. Transitions from ^{26}Mg excited states above 18.4 MeV and below 23 MeV are known to be non-ground state, as established by the present work in combination with that of Wu, Firk, and Berman.[17] These combined results also establish a grouping of the levels of ^{26}Mg, whereby those below about 18 MeV have $T = 1$ and those above 18.4 MeV but below about 23 MeV have $T = 2$. The integrated cross sections are given in Table II and are consistent within experimental errors. The structure observed in the $(\gamma, 2n)$ cross section of ^{26}Mg reflects the same features as seen in the (γ, n) cross section; such structure had not been observed previously.

ACKNOWLEDGMENTS

The authors wish to acknowledge help on the early measurements of these isotopes given by Dr. J. T. Caldwell and Dr. R. L. Bramblett. They also wish to acknowledge informative discussions with Dr. M. S. Weiss, Dr. J. S. O'Connell, and Dr. B. F. Gibson, and the support and encouragement given by Dr. E. Goldberg. They also wish to thank E. Dante and the accelerator operators for their great care and cooperation during the measurements.

---

†Work performed under the auspices of the U. S. Atomic Energy Commission. Preliminary accounts appeared in Bull. Am. Phys. Soc. 10, 541 (1965); 14, 103 (1969); 16, 650 (1971).

*Now at Hewlett Packard Corporation, Palo Alto, California 94304.

[1]E. G. Fuller, H. M. Gerstenberg, and T. M. Collins, *Photonuclear Data Index*, U. S. National Bureau of Standards publications Nos. 277 and 322 (U. S. Government Printing Office, Washington, D. C., 1964); E. Toms, U. S. Naval Research Laboratory, Bibliography No. 31, 1967 (unpublished).

[2]R. C. Bearse, L. Meyer-Schutzmeister, and R. E. Segel, Nucl. Phys. A116, 682 (1968).

[3]R. Nathans and P. F. Yergin, Phys. Rev. 98, 1296 (1955).

[4]J. D. King and W. J. McDonald, Nucl. Phys. 19, 94 (1960).

[5]B. S. Dolbilkin, V. A. Zapevalov, V. I. Korin, L. E. Lazareva, and F. A. Nikolaev, Izv. Akad. Nauk SSSR, Ser. Fiz. 30, 349 (1966) [transl.: Bull. Acad. Sci. USSR, Phys. Ser. 30, 354 (1966)].

[6]J. M. Wyckoff, B. Ziegler, H. W. Koch, and R. Uhlig, Phys. Rev. 137, B576 (1965).

[7]K. Min and W. D. Whitehead, Phys. Rev. 137, B301 (1965).

[8]D. W. Anderson, B. C. Cook, and T. J. Englert, Nucl. Phys. A127, 474 (1969).

[9]B. S. Ishkhanov, I. M. Kapitonov, V. G. Shevchenko, and B. A. Yurev, Izv. Akad. Nauk SSSR, Ser. Fiz. 30, 378 (1966) [transl.: Bull. Acad. Sci. USSR, Phys. Ser. 30, 383 (1966)].

[10]K. Shoda, K. Abe, T. Ishizuka, N. Kawamura, and M. Kimura, J. Phys. Soc. Japan 17, 735 (1965).

[11]E. Spamer, Z. Physik 191, 24 (1966).

[12]O. Titze, E. Spamer, and A. Goldman, Phys. Letters 24B, 169 (1967).

[13]O. Titze, A. Goldmann, and E. Spamer, Phys. Letters 31B, 565 (1970).

[14]C.-P. Wu, Ph.D. thesis, Yale University, 1968 (unpublished).

[15]R. J. Baglan, C. D. Bowman, and B. L. Berman, Phys. Rev. C 3, 672 (1971).

[16]B. L. Berman, R. L. Van Hemert, and C. D. Bowman, Phys. Rev. Letters 25, 386 (1969).

[17]C.-P. Wu, F. W. K. Firk, and B. L. Berman, Phys. Letters 32B, 675 (1970).

[18]S. G. Nilsson, J. Sawicki, and N. K. Glendenning, Nucl. Phys. 33, 239 (1962).

[19]B. Diehl, B. Forkman, and W. Steifler, Nucl. Phys. 56, 615 (1964).

[20]V. G. Neudatchin and V. G. Shevchenko, Phys. Letters 12, 18 (1964).

[21]W. H. Bassichis and F. Scheck, Phys. Letters 19, 509 (1965); Phys. Rev. 145, 771 (1966).

[22]S. C. Fultz, R. L. Bramblett, J. T. Caldwell, and N. A. Kerr, Phys. Rev. 127, 1273 (1962).

[23]J. H. E. Mattauch, W. Thiele, and A. H. Wapstra, Nucl. Phys. 67, 32 (1965).

[24]R. A. Alvarez, B. L. Berman, D. R. Lasher, T. W. Phillips, and S. C. Fultz, University of California Radiation Laboratory Report No. UCRL-73202, 1971 (unpublished).

[25]J. T. Caldwell, R. L. Bramblett, B. L. Berman, R. R. Harvey, and S. C. Fultz, Phys. Rev. Letters 15, 976 (1965).

[26]R. L. Bramblett, J. T. Caldwell, B. L. Berman, R. R. Harvey, and S. C. Fultz, Phys. Rev. 148, 1198 (1966).
[27]P. H. Stelson and L. Grodzins, Nucl. Data A1, 29 (1965).
[28]R. H. Hofstadter, Rev. Mod. Phys. 28, 214 (1956).
[29]B. Block and H. Feshbach, Ann. Phys. (N.Y.) 23, 47 (1963); H. Feshbach, A. K. Kerman, and R. H. Lemmer, *ibid.* 41, 230 (1967).
[30]C. E. Porter and R. G. Thomas, Phys. Rev. 104, 483 (1956).
[31]L. Wilets, *Theories of Nuclear Fission* (Clarendon Press, University of Oxford, Oxford, England, 1964).
[32]B. L. Berman, R. J. Baglan, and C. D. Bowman, Phys. Rev. Letters 24, 319 (1970).
[33]S. Fallieros, B. Goulard, and R. H. Ventner, Phys. Letters 19, 389 (1965).
[34]J. S. O'Connell, B. F. Gibson, and E. Hayward, private communication.

PHYSICAL REVIEW C VOLUME 4, NUMBER 1 JULY 1971

Nuclear Structure of ^{22}Na: The ^{21}Ne(^{3}He,d) Reaction*

J. D. Garrett, R. Middleton, and H. T. Fortune
Physics Department, University of Pennsylvania, Philadelphia, Pennsylvania 19104

(Received 19 February 1971)

The bound states of ^{22}Na have been studied using the ^{21}Ne(^{3}He,d)^{22}Na reaction at a bombarding energy of 18 MeV. Angular distributions of the deuterons have been compared with distorted-wave Born-approximation predictions. The resulting spectroscopic factors are compared with those calculated using the rotational and shell models. (^{3}He,d) spectroscopic factors for $T=1$ final states in ^{22}Na are compared with (d,p) spectroscopic factors from a ^{21}Ne(d,p)^{22}Ne study. The levels of ^{22}Na are discussed in terms of Nilsson configurations and associated rotational bands.

I. INTRODUCTION

^{22}Na is an example of a deformed, odd-odd nucleus. Recent studies indicate that the nuclei in the region of mass 20–24 are among the most deformed nuclei known.[1-5] The rotational model has had considerable success in describing the collective properties of the odd-A and even-even nuclei near mass 22.[6-11] In this model, ^{22}Na is described as a proton and a neutron moving in a prolate deformed potential created by the remaining core nucleons. The low-lying states of ^{22}Na should then correspond to placing the odd proton and neutron in the lowest available Nilsson orbital,[12,13] $\Omega^\pi = \frac{3}{2}^+$, $[Nn_z\Lambda] = [211]$. The energy separation of the resulting 3^+ (ground state) and 0^+ ($E_x = 0.657$ MeV) states have been explained[14,15] in terms of the residual neutron-proton interaction and the Nilsson model. The low-lying states in ^{22}Na have been described as rotational bands based on the $(\frac{3}{2}^+[211])^2$ Nilsson configuration.[1,2,16] A negative-parity band[2,16] has also been suggested. These bands are summarized in Table I.

Experimentally the energy levels of ^{22}Na up to 8 MeV were established by the ^{23}Na(^{3}He, α)^{22}Na and ^{24}Mg(d, α)^{22}Na reactions.[17] The spins, parities, and γ-ray branching ratios of the states of ^{22}Na below 4.2 MeV are known principally from γ-ray decay studies[2,16,18-23] and lifetime measurements.[20,21,23-28] Additional spin-parity assignments were recently made in a study of the ^{20}Ne(^{3}He, p) reaction.[1] The ^{23}Na(p, d) reaction,[29] the ^{23}Na(d, t) reaction,[30,31] and the ^{22}Ne(^{3}He, t) reaction[32] have also yielded information for some of the low-lying levels of ^{22}Na. The previously known spins and parities of ^{22}Na below 5.2 MeV are summarized in Fig. 1.

The single-nucleon stripping reaction has not been performed previously because of the difficulty in preparing a mass-21 target. The stable nucleus of mass 21, ^{21}Ne, is only present as 0.27% of natural Ne and has only recently become available in enrichments >50%. In the present study the ^{21}Ne(^{3}He, d)^{22}Na reaction was performed at an incident energy of 18 MeV using a target of 86.5% ^{21}Ne. The angular distributions of deuteron groups have been compared with distorted-wave Born-approximation (DWBA) predictions. The resulting experimental spectroscopic factors were then compared with predicted spectroscopic factors calculated using Nilsson model and shell-model wave functions.

II. EXPERIMENTAL PROCEDURE AND RESULTS

The ^{21}Ne(^{3}He, d)^{22}Na reaction was studied at an incident energy of 18 MeV using a ^{3}He beam from the University of Pennsylvania tandem Van de Graaff accelerator. Reaction products were momentum analyzed at 12 angles between $7\frac{1}{2}$ and 90°